

New Advances in the Study of Local Structure of Molten Binary Salts

Andrea Di Cicco and Marco Minicucci

Istituto Nazionale di Fisica della Materia, Dipartimento di Matematica e Fisica, Università degli Studi di Camerino, Via Madonna delle Carceri, 62032 Camerino (MC), Italy

Adriano Filipponi

European Synchrotron Radiation Facility, B.P. 220, F-38043 Grenoble, France

(Received 15 May 1996)

Accurate extended x-ray absorption fine structure measurements of molten RbBr and CuBr are analyzed and compared with computer simulations and neutron diffraction results. Advanced multiple-edge *ab initio* methods are used for data analysis. The short-range cation-anion pair distribution function of liquid RbBr is found to be in agreement with previous molecular dynamic simulations confirming the accuracy of present theoretical models. In liquid CuBr, due to the exceptional short-range sensitivity, direct evidence for nearly covalent bonding is obtained, improving previous neutron diffraction determinations. Possible important consequences of present results for experimental studies of binary liquid systems are addressed. [S0031-9007(96)02158-8]

PACS numbers: 61.10.Ht, 61.20.Qg, 61.25.-f, 78.70.Dm

Molten salts are of large applicative interest due to their peculiar thermodynamic, transport, and electrochemical properties, but deserve special attention also from the standpoint of basic physics [1,2]. The microscopic structure of simple ionic liquids has been investigated since a long time using both theoretical and experimental means.

Alkali halides are considered the prototype of ionic bonding, and reliable expressions for the interatomic potentials are currently available. Numerous computer simulations using different techniques were performed for molten alkali halides (see, for example, [1,2] and references therein). On the experimental front, the local structure of several molten alkali chlorides was investigated using neutron diffraction and the isotopic substitution technique (see [3] and list in Ref. [2]). Generally speaking, a good agreement between partial pair distribution functions derived from diffraction measurements, theoretical models, and simulations was achieved.

Several other binary systems are conventionally classified as "mainly ionic," including a few superionic compounds. For example, copper and silver halides show a complex phase diagram in the solid phase and attain rather large values of ionic conductivity before melting occurs. Neutron diffraction (ND) experiments of liquid CuCl and CuBr showed that the local structure differs considerably from those of molten alkali halides. Remarkably enough, since the first pioneering experiment on *l*-CuCl [4], featureless Cu-Cu pair distribution functions were found [4,5]. On the contrary, the halide-halide and Cu-halide distribution functions were found essentially of ionic character. Theoretical explanation of this behavior is still a challenge, although the use of interaction models including the imperfect ionicity of the bond has been attempted [6].

In this Letter, we report the results of accurate multi-edge x-ray absorption experiments on molten RbBr and

CuBr showing that reliable information on local structure of binary liquids and new insights on short-range interactions in the so-called superionic melts can be indeed obtained. As a matter of fact, a few ND experiments using the isotope substitution techniques are available for molten binary systems for a variety of reasons. Quite often, there are practical difficulties in the use of suitable isotopes or mixture of isotopes allowing independent measurements of the partial structure factors. Moreover, the signal-to-noise ratio and the Q extension of some $S(Q)$ measurements are sometimes unsatisfactory. Short-range structural information obtained from accurate EXAFS (extended x-ray absorption fine structure) data can nicely complement previous diffraction measurements and provides a direct experimental test for computer simulations of liquids. Pair distribution functions of liquid RbBr (*l*-RbBr) obtained by molecular-dynamic (MD) simulations [7] are here directly compared for the first time with experimental results. Neutron diffraction results [5] on liquid CuBr (*l*-CuBr) are compared with present experimental data showing the importance and usefulness of performing accurate EXAFS measurements on liquid systems.

The EXAFS spectra were measured at the EXAFS 4 beam line of the Laboratoire Pour l'Utilisation du Rayonnement Electromagnetique (LURE, Orsay) equipped with a double-crystal Si(311) monochromator. Low-noise EXAFS spectra have been recorded at the Br, Cu, and Rb K edges in both solid and liquid phases using sample preparation techniques and high-temperature devices described elsewhere [8]. EXAFS data were analyzed using a novel multiple-edge [9] *ab initio* data-analysis approach based on the GNXAS method [10].

Both solid and liquid phase spectra were analyzed using multiple-scattering (MS) theory and taking account of the well-known background features associated with the [$1s3d$] and [$1s3p$] double-electron excitations in Br and

Rb *K*-edge spectra [11,12]. EXAFS studies of solid CuBr [13] and RbBr [11,14] have been previously reported; here we shall concentrate on structural analysis of *l*-RbBr and *l*-CuBr measured at $T = 730 \pm 5$ and $= 520 \pm 5$ °C.

The EXAFS structural signals $\chi_a(k)$ related to the *a* component (Cu, Rb, or Br) of the RbBr and CuBr binary liquids have been simulated using model partial pair distribution functions $g_{ab}(r)$ and $g_{aa}(r)$ taken from literature. In the case of RbBr the results of a MD computer simulation [7] were used. In Fig. 1, upper part, we compare the experimental Rb and Br *K*-edge $k\chi(k)$ EXAFS signals (Expt) with the results of the simulation (Calc). The residual curves show that the agreement is good although a refinement of the signal can still be attempted.

A very different result is obtained if we calculate the EXAFS signal of CuBr. In this case, a ND experiment was carried out using isotopic substitution of copper and partial $g_{ab}(r)$ functions evaluated. In Fig. 1, lower part, the experimental Rb and Cu *K*-edge EXAFS signals (Expt) are compared with those calculated (Calc) starting from the positive-defined maximum entropy $g_{ab}(r)$ determination [5]. The agreement is very poor. The amplitude of the calculated signal is roughly the same as found in the *l*-RbBr case, but that of the experimental spectrum is at least 5 times bigger (note the change of scale in the figure). A refinement of the short-range structure is clearly necessary.

The refinement of the short-range structure can be carried out using a convenient decomposition of the structural signal $\chi_a(k)$ associated with model partial pair distribution functions,

$$\chi_a(k) = \int_0^\infty dr 4\pi r^2 \rho_b g_{ab}^{(S)}(r) \gamma_{ab}^{(2)}(r, k) + \int_0^\infty dr 4\pi r^2 \rho_a g_{aa}^{(S)}(r) \gamma_{aa}^{(2)}(r, k) + \langle \gamma_{ab}^{(2)}(\text{tail})(k) \rangle + \langle \gamma_{aa}^{(2)}(\text{tail})(k) \rangle + \dots \quad (1)$$

The $\gamma^{(2)}$ terms in Eq. (1) are the irreducible two-body MS signals defined in Ref. [10]. The $g^{(S)}(r)$ functions are short-range well-defined peaks of the partial pair distribution functions, while the effective two-body MS $\langle \gamma_{(\text{tail})}^{(2)} \rangle$ are the result of the average using the tails of the partial distribution functions.

Using the decomposition of Eq. (1), it is possible to perform a reliable refinement of the short-range part $g^{(S)}(r)$ of the radial distribution [9,15,16] using model long-range tails (those of Refs. [5,7] in the present case). Physical constraints on the $g(r)$ shape, related to the correct thermodynamic limit ($k \rightarrow 0$ in the structure factor), have been used in the refinement process of the *l*-RbBr and *l*-CuBr structures.

In Fig. 2 the multiedge best-fit MS calculations (Fit) are compared with the EXAFS experimental spectra (Expt) of *l*-RbBr. The decomposition of the calculated signal is clearly shown in the figure. The dominant signals, $\gamma_{(S)}^{(2)}$ -BrRb and $\gamma_{(S)}^{(2)}$ -RbBr, are those related to the first peak of the $g_{\text{RbBr}}(r)$ distribution function [$g_{\text{RbBr}}(r)$]. The other signals, related to the g_{RbRb} and g_{BrBr} distribution functions and to the tail of the g_{RbBr} one, are comparatively of small amplitude, and we shall not discuss them in detail.

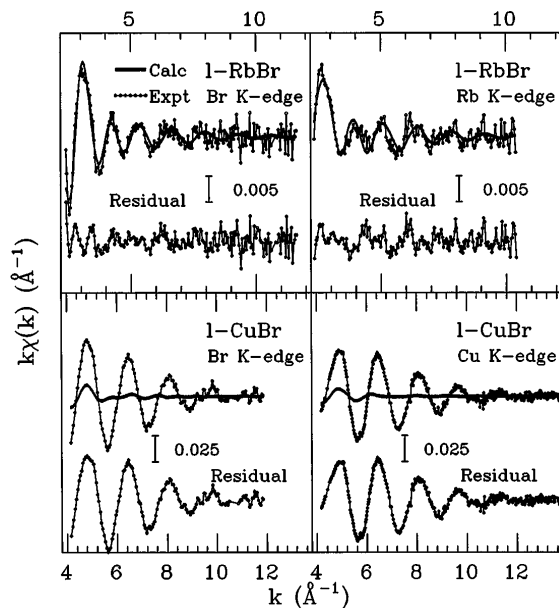


FIG. 1. Experimental EXAFS $k\chi(k)$ spectra (Expt) of *l*-RbBr (upper part) and *l*-CuBr (lower part) compared with calculated signals (Calc) based on computer simulations (*l*-RbBr) and previous diffraction experiments (*l*-CuBr).

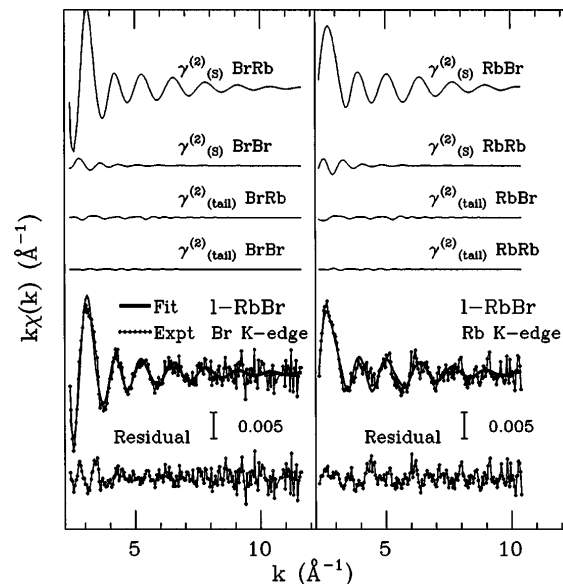


FIG. 2. Best-fit calculated signals associated with the short-range part ($\gamma_{(S)}^{(2)}$) and the tail of the partial distribution functions for *l*-RbBr. The total best-fit curves (Fit) are compared with experimental data (Expt). The agreement is good as shown by the residual curve (bottom).

The overall agreement between experimental and calculated spectra is excellent.

The refined $g_{\text{RbBr}}(r)$ distribution is shown in Fig. 3 (upper panel) and compared with the result of the MD simulation [7]. The shape of the first peak is exactly reproduced, although a shift of about 0.07 \AA toward longer distances is found. The shift is slightly larger than the estimated error bar [9] on the foot of the first $g_{\text{RbBr}}(r)$ peak. The origin of this small discrepancy could be assigned to possible inaccuracies in the short-range part of the interatomic potential. In fact, the importance of including ion polarization in the "rigid-ion" force model was already recognized by the authors in Ref. [7]. However, the overall agreement is very good and this confirms the quality of well established potentials and computer simulation procedures for ionic melts.

The result of the multiedge EXAFS data analysis of *l*-CuBr is shown in Fig. 4. The Cu and Br *K*-edge EXAFS spectra are basically explained by the large amplitude $\gamma_{(s)}^{(2)}$ -CuBr signals associated with the first peak of the $g_{\text{CuBr}}(r)$ distribution function. The quality of the fit is excellent, as shown by the residual curve. There is no evidence of a Cu-Cu signal while a quite small signal related to the $g_{\text{BrBr}}(r)$ is found to contribute to the Br *K*-edge EXAFS. These curves are compatible with previous results on the $g_{\text{CuCu}}(r)$ and $g_{\text{BrBr}}(r)$ distributions. Here we shall discuss in detail only the $g_{\text{CuBr}}(r)$ distribution, for which accurate information has been derived.

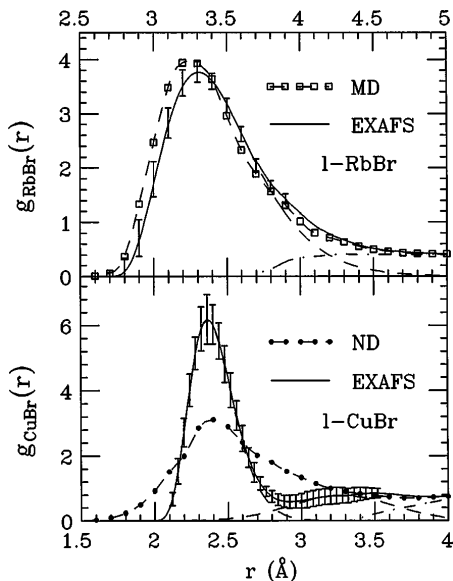


FIG. 3. Upper panel: comparison between the $g_{\text{RbBr}}(r)$ distribution function obtained by EXAFS and that obtained by MD simulations. Lower panel: comparison between previous $g_{\text{CuBr}}(r)$ determination by neutron diffraction (ND) and present EXAFS refinement. Dashed and dot-dashed curves are the short-range part and the tail of the distribution functions. The error bars indicate the estimated accuracy of the EXAFS refinements.

The reconstructed $g_{\text{CuBr}}(r)$ of *l*-CuBr is shown in Fig. 3, lower panel, and it is compared with that determined using ND. The EXAFS $g_{\text{CuBr}}(r)$ shows a narrower well-defined first-neighbor peak (FWHM $\sim 0.3 \text{ \AA}$). The remarkable difference between the EXAFS and ND determinations should not surprise the reader. The sharper $g_{\text{CuBr}}(r)$ is perfectly compatible with the original ND data [5], within the noise level. In Fig. 5 we compare the experimental $S_{\text{CuBr}}(Q)$ ND measurement with the curve obtained through back transformation from the $g_{\text{CuBr}}(r)$ refined using EXAFS data, and with the original $S(Q)$ derived in Ref. [5] using the maximum-entropy method. It is clear that the EXAFS and maximum-entropy curves are both compatible with experimental data within the noise level, as confirmed by χ^2 analysis. These two curves, however, correspond to remarkably different short-range $g_{\text{CuBr}}(r)$ curves as shown in Fig. 3. By comparison the corresponding EXAFS signals differ by nearly 1 order of magnitude as shown in Fig. 1 (lower panels). This is a typical case in which very precise structural information can be gained by EXAFS experiments taking advantage of the exceptional short-range sensitivity. In comparison, the ND investigation is limited by the low contrast in the isotopes scattering lengths that, with a few exceptions, is a rather general occurrence.

Present findings on *l*-CuBr shed some light on the debate on the nature of the like-unlike ion interaction in "superionic" melts, and, of course, are likely to be extended to the CuCl case, usually considered as reference compound for "superionic" melts. In fact, it is now clear that a simple ionic interatomic potential

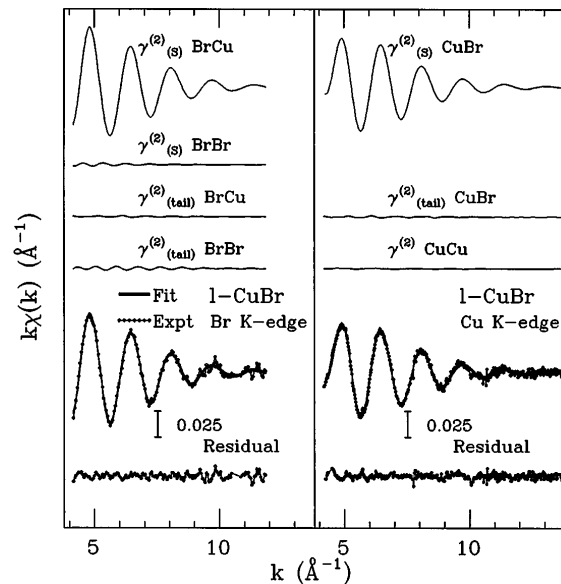


FIG. 4. Best-fit calculated signals associated with the short-range part ($\gamma_{(s)}^{(2)}$) and the tail of the partial distribution functions for *l*-CuBr. The total best-fit curves (Fit) are compared with experimental data (Expt). The agreement is excellent as shown by the residual curve (bottom).

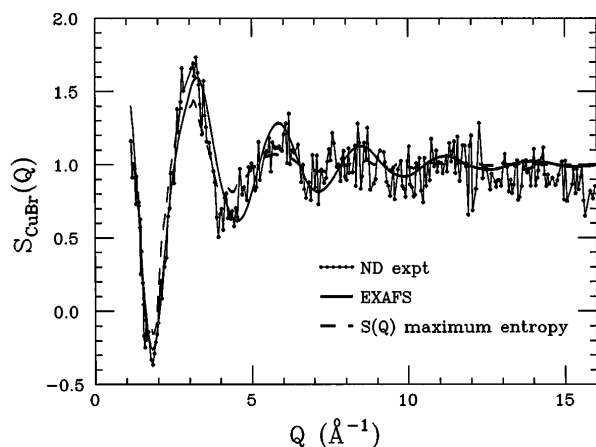


FIG. 5. Comparison of the partial structure factor $S_{\text{CuBr}}(Q)$ as derived by neutron diffraction (ND expt) [5], analyzed using the maximum-entropy method (dashed), [5] and the $S(Q)$ derived by present EXAFS experiment.

cannot account for the observed shape of the first peak of the $g_{\text{CuBr}}(r)$, which instead suggests the existence of nearly covalent bonds [17]. The coordination number defined by the first peak is 3.0 (3), to be compared with fourfold coordination of solid CuBr. While *l*-CuBr cannot be simply considered a molecular liquid, it is clear that theoretical models including nonionic interactions should be devised to explain the experimental $g_{\text{CuBr}}(r)$. New theoretical investigations are thus stimulated by present work.

The results presented in this Letter have two important consequences. First, they demonstrate that EXAFS, provided that accurate experiments and proper data analysis are carried out, can give very accurate structural information useful for testing interatomic potentials and complementary to results obtained by other spectroscopies on liquid systems. In particular, several liquid binary systems for which ND diffraction measurements are difficult to perform can now be studied using multiple-edge EXAFS. Second, present data on *l*-CuBr are found to provide new and reliable information on the partial $g_{\text{CuBr}}(r)$ distri-

bution function, improving our knowledge on fundamental processes in the so-called “superionic” melts which represent an example of transition between ionic and non-ionic liquids.

-
- [1] N. H. March and M. P. Tosi, *Coulomb Liquids* (Academic Press, London, 1984).
 - [2] M. Rovere and M. P. Tosi, *Rep. Prog. Phys.* **49**, 1001 (1986).
 - [3] F. G. Edwards, J. E. Enderby, R. A. Howe, and D. I. Page, *J. Phys. C* **8**, 3483 (1975); S. Biggin and J. E. Enderby, *J. Phys. C* **15**, L305 (1982).
 - [4] D. I. Page and K. Mika, *J. Phys. C*, **4**, 3034 (1971); S. Eisenberg, J.-F. Jal, J. Depuy, P. Chieux, and W. Knoll, *Philos. Mag. A* **46**, 195–209 (1982).
 - [5] D. A. Allen and R. A. Howe, *J. Phys. Condens. Matter* **4**, 6029–6038 (1992).
 - [6] M. Ginoza, J. H. Nixon, and M. Silbert, *J. Phys. C* **20**, 1005 (1987); J. Trullàs, A. Giró, J. A. Padró, and M. Silbert, *Physica (Amsterdam)* **171A**, 384 (1991).
 - [7] J. R. D. Copley and A. Rahman, *Phys. Rev. A* **13**, 2276 (1976).
 - [8] A. Filipponi and A. Di Cicco, *Nucl. Instrum. Methods Phys. Res., Sect. B* **93**, 302 (1994).
 - [9] A. Di Cicco, *Phys. Rev. B* **53**, 6174 (1996).
 - [10] A. Filipponi, A. Di Cicco, and C. R. Natoli, *Phys. Rev. B* **52**, 15 122 (1995). The acronym GNXAS derives from g_n (the n -body distribution functions) and XAS (x-ray absorption spectroscopy).
 - [11] G. Li, F. Bridges, and G. S. Brown, *Phys. Rev. Lett.* **68**, 1609 (1992).
 - [12] P. D’Angelo, A. Di Cicco, A. Filipponi, and N. V. Pavel, *Phys. Rev. A* **47**, 2055 (1993).
 - [13] J. B. Boyce, T. M. Hayes, and J. C. Mikkelsen, Jr., *Phys. Rev. B* **23**, 2876 (1981).
 - [14] A. Frenkel, E. A. Stern, M. Qian, and M. Newville, *Phys. Rev. B* **48**, 12 449 (1993).
 - [15] A. Filipponi, *J. Phys. Condens. Matter* **6**, 8415 (1994).
 - [16] A. Filipponi and A. Di Cicco, *Phys. Rev. B* **51**, 12 322 (1995).
 - [17] J. G. Powles, *J. Phys. C* **8**, 895 (1975).